ELSEVIER

Journal of Power Sources 55 (1995) 19–24

JOURNAL OF POWER SOURCES

Characterization of anodic films on lead and lead alloys by impedance spectroscopy

S. Brinić [a], M. Metikoš-Huković [b], R. Babić [b]

[a] *Faculty of Technology, University of Split, N. Tesle 10, 58000 Split, Croatia*

[b] *Department of Electrochemistry, Faculty of Chemical Engineering and Technology, University of Zagreb, Savska 16, PO Box 177, 41000 Zagreb, Croatia*

Received 5 August 1994; revised 19 October 1994

Abstract

The behaviour of lead and lead–antimony binary alloys with 1.3–4.5 wt.% antimony was investigated in the lead sulfate and lead oxide potential regions by means of cyclic voltammetry and electrochemical impedance spectroscopy. The impedance data show that the inner PbO barrier layer is formed beneath the initially grown $PbSO_4$ porous layer at potentials positive to −0.2 V versus SCE. The antimony content influences the characteristics of the anodic layer by decreasing its resistance and increasing its capacity. These changes were observed both on the lead sulfate and especially the lead oxide layers. With increased anodic polarization, the film resistance increases as well while the capacity shows the opposite change.

Keywords: Lead; Lead–antimony alloys; Lead/acid batteries; Impedance spectroscopy

1. Introduction

Solid state processes at passive layers formed on lead in sulfuric acid solution have been studied extensively in recent years [1–4]. Lead corrosion appears to be a rather complex phenomenon as the structure and composition of films formed on metal surfaces depend on a large number of variables. Despite the great efforts already made, the influence of electrode potential on the characteristics and properties of the passive film on lead is still a subject of discussion. On the basis of X-ray diffraction and electrochemical measurements, Pavlov [1,2] suggested that the nature of the passive film formed on lead electrodes in sulfuric acid solution can be separated into three distinct potential regions. The passive layer formed at potentials from −0.62 to −0.05 V (−0.97 to −0.40 V versus Hg/Hg_2SO_4) consists of $PbSO_4$ crystals. The layer produced from −0.05 to 1.3 V (−0.40 to 0.95 V versus Hg/Hg_2SO_4) is composed of $PbSO_4$ and an inner layer involving several basic lead compounds (mainly tetra-PbO and basic lead sulfates), which builds up progressively beneath the initial $PbSO_4$ porous layer structure. At potentials more positive than 1.3 V (0.95 V versus Hg/Hg_2SO_4) α- and β-PbO_2 become the predominant anodic oxide products.

Formation of PbO has been confirmed by X-ray diffraction analysis [5,6], sensitive voltammetric measurements [7–9], photo-current measurements [10,11], laser Raman spectroscopy [12] and impedance measurements [13] underneath the semipermeable $PbSO_4$ layer at potentials positive to ~ −0.05 V. However, the potential at which PbO formation is detected depends on the technique used. Recently, while investigating the reduction process of PbO film on the lead electrode in sulfuric acid solution, Gou [14] has found that tetra-PbO can be formed at the potential positive to −0.20 V (−0.55 V versus Hg/Hg_2SO_4). It seems that the potential differences observed are caused by a slow solid-state mechanism by which PbO is formed.

It has been established that antimony, widely used as an alloying additive in lead alloys for casting lead/acid battery grids, not only significantly affects the casting and the mechanical properties of the alloys, but also has a strong impact on the electrochemical processes at the positive plate of the battery. Therefore its influence on the electrochemical behaviour of lead in Pb–Sb alloys in sulfuric acid solution has been extensively studied [15].

Antimony oxidation in Pb–Sb alloys begins at the potential values at which PbO formation takes place under the $PbSO_4$ perm-selective membrane [8,16–18],

SSDI 0378-7753(94)02151-R

the properties of which greatly influence the potential–current profile corresponding to antimony oxidation [19].

It is believed that antimony oxidation in alloys changes the composition of the anodic layer; simultaneously to the formation of lead-oxide compounds (PbO, non-stoichiometric PbO_n ($1<n<2$) and PbO_2), substituted $Pb_{1-x}Sb_xO$, non-stoichiometric $Pb_{1-x}Sb_xO_n$, and $Pb_{1-x}Sb_xO_2$ may be formed [20]. Due to the antimony oxidation, the anodic layer on Pb–Sb alloys is more porous than the one formed on pure lead. This promotes the formation of basic lead sulfates because SO_4^{2-} ions can easily pass through the porous layer of $PbSO_4$. A thicker layer of basic lead sulfates on Pb–Sb electrodes reduces the potential gradient and thus slows the migration rates of H^+ and OH^- ions and hinders the growth of the tetra-PbO layer [21,22]. As a consequence, an increase in conductivity of the corrosion layer on Pb–Sb alloys compared to the pure lead electrode has been observed [9,15,23].

In our previous studies [9,19] the influence of antimony on the kinetics and mechanisms of various redox processes on Pb–Sb alloys (Sb content 1.3–4.5 wt.%) in sulfuric acid solution was investigated by means of voltammetry techniques. Impedance measurements performed in the potential region of antimony oxidation showed a decrease in polarization resistance and an increase in layer capacitance with increasing antimony content in the alloy [9]. The aim of the present work is to investigate the influence of antimony on the properties of the anodic layer formed on Pb–1.3–4.5% Sb alloys in 0.5 M sulfuric acid solution in a wider potential range. For the sake of comparison, the electrochemical properties of the anodic layer on pure lead has been also investigated.

2. Experimental

The investigation was performed on pure lead (99.998 wt.%) and Pb–Sb alloys with antimony content of 1.3, 2.75, 3.75 and 4.5 wt.%, by means of cyclic voltammetry (CV) and electrochemical impedance spectroscopy (EIS). Scanning electron microscope examination of the structure and morphology of lead and Pb–Sb alloys was also carried out. The electrodes had a cylindrical form. The lateral surface of the cylinder was insulated by Araldite, exposing only the cylinder base plane to the solution; the surface area was 0.283 cm^2. Before each experiment the electrodes were polished with silicon carbide grinding paper (grit 600), degreased in trichloroethylene, rinsed with distilled water, and, prior to each measurement, polarized for 10 min at −1.0 V, below the equilibrium potential of the $Pb/PbSO_4$ couple, to remove oxides formed on the surface due to contact with air, and $PbSO_4$ formed during the immersion.

The experiments were performed in a standard two-compartment glass cell at 298 K using aqueous 0.5 M H_2SO_4 solution as the electrolyte. The counter electrode was a large platinum plate, and the reference electrode was a saturated calomel electrode (SCE). All potential values in the paper are reported versus the SCE.

Measurements were performed using an EG&G Princeton applied research model 273 potentiostat, and an EG&G model 5315 lock-in amplifier controlled by an IBM PC computer. Impedance measurements were performed in the frequency range 30 mHz–100 kHz with the a.c. voltage amplitude ±5 mV.

3. Results and discussion

3.1. Cyclic voltammetry on lead–antimony alloys

Fig. 1 represents the current–potential curve for an Pb–Sb alloy with 3.7 wt.% Sb in a 0.5 M sulfuric acid solution. Well-defined current maxima corresponding to oxidation and reduction processes of lead, antimony and their compounds [8,9,16–19] can be seen. Almost the same voltammogram shape was obtained on Pb–Sb alloys with antimony content of 1.3, 2.7 and 4.5 wt.%. A more detailed analysis of these voltammograms has been given elsewhere [9,19]. In short, the potential sweep in the positive direction first shows peak A_1 corresponding to formation of a $PbSO_4$ layer. Antimony oxidation (current peak A′) begins in the PbO potential region under the $PbSO_4$ perm-selective membrane. The height of peak A′ increases with increased antimony content. Antimony oxidation in the alloy changes the composition of the anodic layer [15]. Pavlov et al. [20] have proposed the formation of substituted Pb–Sb oxide species. Increased anodic current above 1.8 V signifies both oxidation of $PbSO_4$ to β-PbO_2, which is the stable phase in acid solution, and evolution of oxygen.

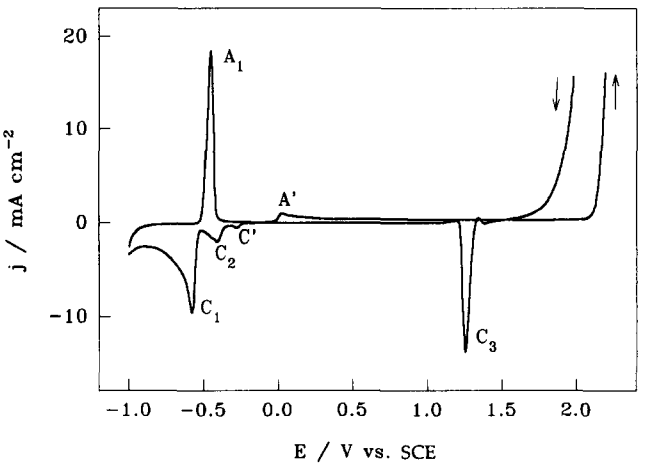

Fig. 1. Cyclic voltammogram on a Pb–3.5 wt.% Sb electrode in a 0.5 M H_2SO_4 solution; sweep rate 10 mV s^{-1}.

The complexity of the voltammetric peaks in the early part of reversed potential sweep is caused by simultaneous cathodic and anodic reactions that occur in this potential range. These are the PbO_2 discharge (peak C_3) and oxidation of the lead substrate and/or some incompletely oxidized products of lead. The current peak C′ corresponds to reduction of Sb(III) to Sb. It becomes higher with increased antimony content. Cathodic peak C_2, which appears at −0.47 V corresponds to the reduction of tetra-PbO and basic lead sulfates [22,24,25]. Its height decreases with increased antimony content in the alloy. At potentials lower than ~ −0.55 V, $PbSO_4$ reduction occurs, which is reflected in cathodic peak C_1.

3.2. Electrochemical impedance spectroscopy data

3.2.1. Impedance data on pure lead

The impedance spectra obtained on lead electrodes in 0.5 M H_2SO_4 solution were found to depend on the film formation potential. Figs. 2 and 3 show Nyquist diagrams corresponding to the impedance of lead at different potentials in the potential range between $PbSO_4$ formation and oxygen evolution.

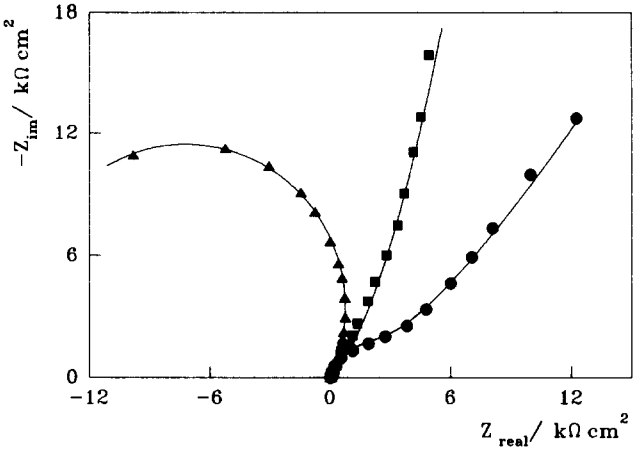

Fig. 2. Nyquist plots for a Pb electrode in a 0.5 M H_2SO_4 solution at: ▲, −0.45; ■, −0.40; ●, −0.30 V vs. SCE.

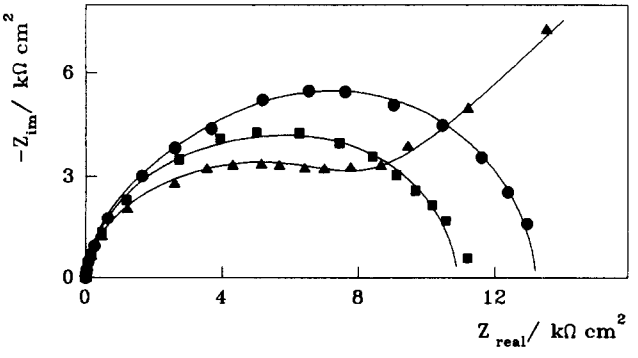

Fig. 3. Nyquist plots for a Pb electrode in a 0.5 M H_2SO_4 solution at: ▲, −0.20; ■, 0.00; ●, 0.20 V vs. SCE.

The shape of the impedance spectra obtained at potentials $E_i \leqslant -0.3$ V (Fig. 2) exhibits a distorted capacitive semicircle at high frequencies and a second contribution related to a slow process which, at decreasing frequency and potential, tends towards a negative value for the polarization resistance $R_p = \lim_{f \to 0}[Z(j\omega)]$. This behaviour is consistent with the negative slope of the polarization curve obtained for the system in this potential range (Fig. 1). Similar observations have been reported by Varela et al. [13] for lead electrodes in 5 M H_2SO_4 solution. The impedance spectrum obtained at −0.2 V (Fig. 3) exhibits a high frequency loop and a low frequency linear part with a slope which is almost exactly 45°, being the characteristic phase angle of a Warburg impedance.

The impedance spectra obtained at $E_i \geqslant 0.0$ V (Fig. 3) exhibit only capacitive semicircles. Fig. 3 shows that the impedance spectra obtained at $E_i \geqslant -0.2$ V are depressed. Deviations of this kind, often referred to as frequency dispersion, have been attributed to inhomogeneities of the solid surfaces. A practical way to represent distributed processes such as corrosion of a rough and inhomogeneous electrode is with an element that follows its distribution such as a constant phase element (CPE). The CPE impedance takes the form [26]:

$$Z_{CPE} = (Q(j\omega)^n)^{-1} \quad (1)$$

where coefficient Q is a combination of properties related to both surface and electroactive species. The exponent n ranges between −1 and 1. The value of −1 is characteristic of an inductor, the value of 1 corresponds to a capacitor, the value of 0 corresponds to a resistor and the value of 0.5 can be assigned to diffusion phenomena.

The equivalent circuits which have given the best fitting procedure of the experimental data obtained at $E_i \geqslant -0.3$ V are presented in Fig. 4. They consist of CPE Q_1 ($n=1$, $Q=C$) in parallel to series resistor R_1

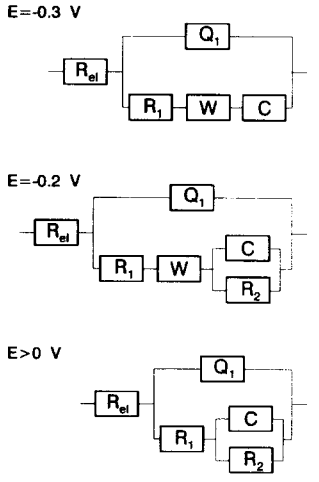

Fig. 4. Equivalent circuits used to fit experimental data.

and the Warburg impedance and capacitance C in parallel to R_2. R_{el} corresponds to the electrolyte resistance. For impedance spectra obtained at $E_i \geqslant 0.0$ V the Warburg impedance was omitted. The best fitting procedure of the high-frequency capacitive loop obtained at -0.30 V was achieved with one time constant. The values of the equivalent circuit elements calculated for all spectra which were measured at $E_i \geqslant -0.3$ V are listed in Table 1.

Under the assumption that the single time constant corresponds to a single $PbSO_4$ layer and the two time constants to a composite $PbSO_4$ + oxide layer, it follows that the anodic film on lead in a 0.5 M H_2SO_4 solution corresponds to a single sulfate layer at potentials negative to -0.2 V and a composite $PbSO_4$ + oxide layer at potentials positive to -0.2 V. The diffusion process observed at potentials up to -0.2 V could be attributed to the migration of H^+ ions from the inner layer to the bulk solution and OH^- ions in the opposite direction. Accordingly, R_1 and R_2 correspond to the resistance of the outer and inner parts of the anodic layer, respectively. A slow change in R_1 and a more rapid change in R_2 seems to be logical and plausible. The results obtained are consistent with the data reported by Gou [14] according to which the formation of tetra-PbO underneath the $PbSO_4$ perm-selective membrane occurs at potentials positive to -0.2 V.

A similar approach has been used by Varela et al. [13] for impedance results obtained on pure lead in 5 M H_2SO_4 solution but the potential at which formation of tetra-PbO occurs was found to be more positive.

It was found that the impedance spectra obtained on lead electrodes in 0.5 M H_2SO_4 solution depend on the time of polarization. Fig. 5 shows the Nyquist plot corresponding to the impedance of the lead electrode after 20, 40 and 120 min of polarization at -0.2 V. The fitting procedure of the experimental data performed by using the equivalent circuit in Fig. 4 yields parameters which are listed in Table 2. An increase in resistance and decrease in capacitance with the time of polarization can be observed.

Table 1
Fit parameters for a Pb electrode in 0.5 M H_2SO_4 at different potentials

	Potential (mV)			
	−300	−200	0	200
R_{el} (Ω cm^2)	0.56	1.19	1.18	1.00
Q (Ω^{-1} cm^{-2} s$^n \times 10^{-6}$)	3.96	6.86	6.90	4.60
n	0.914	0.926	0.922	0.936
R_1 (Ω cm^2)	2654	5609	8362	8473
W (Ω^{-1} cm^{-2} s$^{0.5} \times 10^{-4}$)	0.87	2.21		
C (μF cm^{-2})	725	47	39.3	11
R_2 (Ω cm^2)		1378	2544	4731

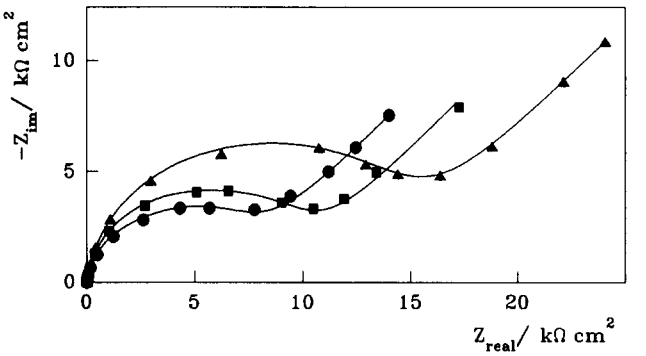

Fig. 5. Nyquist plots for a Pb electrode in a 0.5 M H_2SO_4 solution at -0.2 V vs. SCE after: ●, 20; ■, 40; ▲, 120 min of polarization.

Table 2
Fit parameters for a Pb electrode at different polarization times at -0.2 V vs. SCE in 0.5 M H_2SO_4

	t (min)		
	20	40	120
R_{el} (Ω cm^2)	1.19	1.2	1.20
Q_1 (Ω^{-1} cm^{-2} s$^n \times 10^{-6}$)	6.86	3.44	3.01
n	0.926	0.930	0.925
R_1 (Ω cm^2)	5609	7988	11835
W (Ω^{-1} cm^{-2} s$^{0.5} \times 10^{-4}$)	2.21	2.05	1.53
C (μF cm^{-2})	47.0	41.6	27.0
R_2 (Ω cm^2)	1378	1421	1987

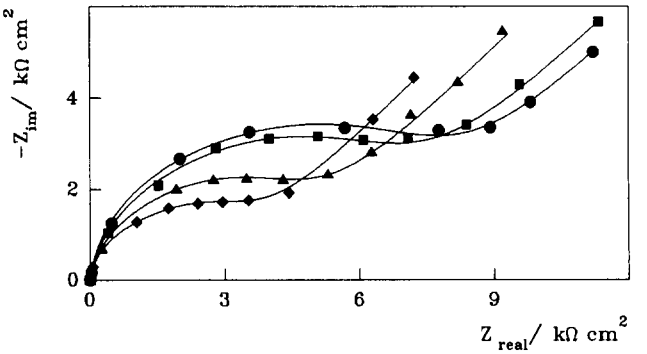

Fig. 6. Nyquist plots for (●) Pb and Pb–Sb alloys: ■, 1.3; ▲, 2.7; ◆, 3.7 wt.% in a 0.5 M H_2SO_4 solution at -0.2 V vs. SCE.

3.2.2. *Impedance data on Pb–Sb alloys*

The impedance spectra for Pb–Sb alloys were measured in the potential region where the anodic film was expected to be composed of $PbSO_4$ and oxide layers, e.g. at potentials $E_i \geqslant -0.2$ V. Fig. 6 shows the Nyquist diagrams corresponding to the impedance of Pb–Sb alloys in 0.5 M H_2SO_4 solution at -0.2 V. For the sake of comparison the impedance spectra of pure lead is also represented. The spectra, of the same shape as the one for pure lead, include a high frequency loop and a low frequency linear part with a slope which is almost exactly 45°, being characteristic of the Warburg impedance. Parameters calculated by using the equiv-

alent circuit in Fig. 4 are listed in Table 3. The analogy between the equivalent circuit elements obtained for lead and Pb–Sb alloys suggests a similar interpretation, e.g. the two-layer structure of the anodic film. In spite of the fact that Sb does not take part in the electrochemical process at −0.2 V, the results obtained show that the resistance values slightly decrease, while the capacitance values increase with an increase of the Sb content in the alloy.

Impedance spectra obtained on Pb–Sb alloys in the potential region in which antimony oxidation takes place ($E_i \geqslant 0.0$ V) are of the same shape as the spectra of pure lead (see Fig. 3). The spectra exhibit a capacitive contribution and the capacitative loop diminishes with the increase of the antimony content in the alloy. The impedance spectra were fitted by using the equivalent circuit in Fig. 4, and the values of the equivalent circuit elements obtained are listed in Table 4.

The resistance and capacitance values presented in Tables 3 and 4 can be correlated with the outer $PbSO_4$ layer and inner oxide layer as shown for pure lead [13] and Pb–Sb alloys at higher anodic potential ($E_i = 0.2$ V) [9]. Data obtained show that the properties of the sulfate layer remain almost constant during anodic polarization, while oxide layer properties change considerably. Tables 3 and 4 also show that alloying lead with antimony decreases the resistance of both the sulfate and oxide layers on Pb–Sb alloys, and with the increase of the antimony content the layer resistance decreases. This observation is in accordance with cyclic voltammetry results, and confirms literature results [9,15,23,27,28].

Table 3
Fit parameters for Pb and Pb–Sb electrodes in 0.5 M H_2SO_4 at −0.2 V vs. SCE

	Sb content (%)			
	0	1.3	2.7	3.7
R_{el} (Ω cm^2)	1.19	0.82	0.65	0.80
Q_1 (Ω^{-1} cm^{-2} s$^n \times 10^{-6}$)	6.86	9.27	13.81	16.85
n	0.926	0.905	0.906	0.923
R_1 (Ω cm^2)	5609	5168	3588	2454
W (Ω^{-1} cm^{-2} s$^{0.5} \times 10^{-4}$)	2.21	2.40	3.11	3.83
C (μF cm^{-2})	47.0	50.2	71.2	106.2
R_2 (Ω cm^2)	1378	1211	809	726

Table 4
Fit parameters for Pb and Pb–Sb electrodes in 0.5 M H_2SO_4 at 0.0 V vs. SCE

	Sb content (%)				
	0	1.3	2.7	3.7	4.5
R_{el} (Ω cm^2)	1.18	1.14	1.15	1.01	1.00
Q_1 (Ω^{-1} cm^{-2} s$^n \times 10^{-6}$)	6.90	9.9	12.1	14.2	14.7
n	0.922	0.910	0.877	0.859	0.873
R_1 (Ω cm^2)	8362	8071	6823	5171	5044
R_2 (Ω cm^2)	2544	1650	891	744	718
C (μF cm^{-2})	39.3	93.0	143	471	494

4. Conclusions

The electrochemical behaviour of Pb and Pb–Sb binary alloys with antimony content of 1.3–4.5 wt.% was studied in the potential regions of $PbSO_4$ and PbO formation. The investigation was performed in 0.5 M H_2SO_4 solution by means of cyclic voltammetry and electrochemical impedance spectroscopy techniques.

The results obtained show that the inner PbO barrier layer beneath the initially grown $PbSO_4$ on the lead electrode is formed at potentials positive to −0.2 V versus SCE. The properties of both layers, the inner PbO and the outer $PbSO_4$ (their resistance and capacitance), are potential and time dependent. With the increase of anodic polarization and ageing time, the layer resistance increases while its capacitance decreases.

Alloying lead with antimony influences the electrical properties of the anodic layer; an increase in capacitance and a decrease in resistance are caused by increased antimony in the alloy. These changes were observed on both the outer $PbSO_4$ and inner PbO layer, the latter being more considerably influenced. The antimony content in the alloy influences the characteristics of the anodic layer, even in the potential region prior to oxidation of antimony.

References

[1] D. Pavlov, *Electrochim. Acta, 23* (1978) 845.
[2] D. Pavlov, *J. Electroanal. Chem., 118* (1981) 167.
[3] D. Pavlov and Z. Dinev, *J. Electrochem. Soc., 127* (1975) 845.
[4] D. Pavlov, *J. Electrochem. Soc., 139* (1992) 3075.
[5] D. Pavlov, C.N. Poulieff, E. Klaja and N. Iordanov, *J. Electrochem. Soc., 116* (1969) 316.
[6] D. Pavlov and N. Iordanov, *J. Electrochem. Soc., 117* (1970) 1103.
[7] J.P. Carr, N.A. Hampson and R. Taylor, *J. Electroanal. Chem., 33* (1971) 109.
[8] J.C. Chang, M.M. Wright and E.M.L. Valeriste, in D.H. Collins (ed.), *Power Sources 6,* Academic Press, New York, 1977, p. 69.
[9] R. Babić, M. Metikoš-Huković, N. Lajqy and S. Brinić, *J. Power Sources, 52* (1994) 17.
[10] D. Pavlov, S. Zanova and G. Papazov, *J. Electrochem. Soc., 124* (1977) 1522.
[11] J.S. Buchanan, N.P. Freestone and L.M. Peter, *J. Electroanal. Chem., 182* (1985) 383.
[12] K.R. Bullock, *J. Electroanal. Chem., 222* (1987) 347.
[13] F.E. Varela, L.M. Gassa and J.R. Vilche, *J. Electroanal. Chem., 353* (1993) 147.
[14] Y. Guo, *J. Electrochem. Soc., 138* (1991) 1222.

[15] T. Laitinen, K. Salmi, S. Sundholm, B. Monahov and D. Pavlov, *Electrochim. Acta, 36* (1991) 605.
[16] H.S. Pensar, in D.H. Collins (ed.), *Power Sources 3,* Oriel, Newcastle-upon-Tyne, UK, 1971, p. 79.
[17] T.F. Sharpe, *J. Electrochem. Soc., 124* (1977) 168.
[18] B.K. Mahato, *J. Electrochem. Soc., 126* (1979) 365.
[19] M. Metikoš-Huković, R. Babić and S. Omanović, *J. Electroanal. Chem., 347* (1994) 199.
[20] D. Pavlov and B. Monahov, *J. Electroanal. Chem., 305* (1991) 57.
[21] Y. Guo, *J. Electrochem. Soc., 139* (1992) 2114.
[22] Y. Guo, J. Yue and C. Liu, *Electrochim. Acta, 38* (1993) 1131.
[23] M.P.J. Brennan, B.N. Stirrup and N.A. Hampson, *J. Appl. Electrochem., 4* (1974) 497.
[24] Y. Guo, *J. Electrochem. Soc., 140* (1993) 3369.
[25] Y. Guo, *J. Electroanal. Chem., 345* (1993) 377.
[26] J.R. Macdonald, *J. Electroanal. Chem., 223* (1987) 25.
[27] M.N. Ijomah, *J. Electrochem. Soc., 134* (1987) 1960.
[28] S. Webster, P.J. Mitchell, N.A. Hampson and D.I. Dyson, *J. Electrochem. Soc., 133* (1986) 137.